

# Article type: Paper

- August 17, 2016
- ~6500 words (Introduction to Conclusions). Nine (9) Tables and nine (9) Figures.



## Manufactured Aggregate from Cement Kiln Dust

### Author 1

- Craig Lake, Ph.D, P.Eng.
- Professor, Department of Civil and Resource Engineering, Dalhousie University, Halifax, Canada,

### Author 2

- Hun Choi, MASc
- Department of Civil and Resource Engineering, Dalhousie University, Halifax, Canada
- Currently PhD Candidate, Dalhousie University, Halifax, Canada

### Author 3

- Colin D Hills, CSci, DIC, Ph.D, MIMMM, FGS
- Professor, Department of Engineering Science, Greenwich University, Kent, United Kingdom

### Author 4

- Peter Gunning, Ph.D
- Visiting Lecturer, Department of Engineering Science, Greenwich University, Kent, United Kingdom

### Author 5

- Idris Manaqibwala, BEng.
- Former undergraduate research student, Department of Civil and Resource Engineering, Dalhousie University, Halifax, Canada
- Currently Officer Trainee at Hindustan Petroleum Co. Ltd., India

### Corresponding Author

Craig Lake

Department of Civil and Resource Engineering

Dalhousie University, Sexton Campus

1360 Barrington St., Rm 214 Bld. D

Halifax, NS, Canada B3H 4R2

[craig.lake@dal.ca](mailto:craig.lake@dal.ca)

1  
2 **Abstract**

3 This paper presents the results of a laboratory study that evaluates the geotechnical and geo-  
4 environmental properties of a manufactured aggregate derived from a cement kiln dust (CKD).  
5 The aggregate manufacturing process involves accelerated carbonation technology (ACT),  
6 which has been used to treat contaminated soils at trial-scale. The process is operating at  
7 commercial scale in the United Kingdom, producing aggregate from thermal residues. The ACT  
8 process relies on the accelerated reaction of carbon dioxide with the calcium oxide in the CKD  
9 material in the presence of water. No additional binder is used in this study, instead relying  
10 solely on the formation of carbonate to form the aggregate.  
11  
12  
13  
14  
15  
16

17 In this paper, the aggregate manufacturing process is briefly described. To explore future  
18 potential construction applications of the aggregate, several geotechnical test results are used  
19 to assess strength and durability (i.e. individual particle strength, internal shear strength of the  
20 particle assemblage, wet/dry testing, freeze/thaw testing). Screening tests for the aggregate's  
21 geo-environmental characteristics are discussed (metal leaching, dissolved heavy metal  
22 adsorption and hydraulic conductivity) to further assess potential uses. It is shown that the  
23 aggregate studied has adequate properties for a variety of construction applications, but is  
24 unsuitable for use in freezing and thawing environments.  
25  
26  
27  
28  
29  
30  
31  
32  
33

34 **Keywords**

35  
36 Ash utilization, Contaminated material, Strength and testing of materials  
37  
38  
39  
40  
41  
42  
43  
44  
45  
46  
47  
48  
49  
50  
51  
52  
53  
54  
55  
56  
57  
58  
59  
60  
61  
62  
63  
64  
65

## List of Notation

1  
2 ACT is Accelerated Carbonation Technology  
3 CID is consolidated isotropic drained  
4  $C_c$  is coefficient of curvature  
5  $C_u$  is coefficient of uniformity  
6 CKD is cement kiln dust  
7 D is aggregate diameter  
8  $D_{10}$  is aggregate diameter at which 10 percent of sample is finer  
9  $D_{30}$  is aggregate diameter at which 30 percent of sample is finer  
10  $D_{60}$  is aggregate diameter at which 60 percent of sample is finer  
11 SP is poorly graded sand  
12 ICP-OES is inductively coupled plasma optical emission spectrometry  
13 ICP-MS is inductively coupled plasma mass spectrometry  
14 LOI is loss on ignition  
15 S is compressive strength of aggregate  
16 SSD is saturated surface dry  
17 XRF is x-ray fluorescence  
18 WP-XRF is wavelength dispersion Fluorescence  
19 MIP is Mercury intrusion porosimetry  
20 P is absolute pressure  
21  $T_s$  is surface tension  
22  $\theta$  is contact angle between the mercury and the soil  
23  $\phi$  is the drained internal angle of friction  
24 LVDT is linear variable differential transformer  
25 PC is failure load of the individual aggregate  
26  $\sigma'_{1f}$  is maximum effective major principal stress at failure  
27  $\sigma'_{3f}$  is maximum effective minor principal stress at failure  
28  
29  
30  
31  
32  
33  
34  
35  
36  
37  
38  
39  
40  
41  
42  
43  
44  
45  
46  
47  
48  
49  
50  
51  
52  
53  
54  
55  
56  
57  
58  
59  
60  
61  
62  
63  
64  
65

## 1. Introduction

Accelerated carbonation technology (ACT) utilises fine-grained mineral and waste materials in the production of engineering products, including lightweight and relatively low strength aggregates (Gunning et al., 2009). The process is patented for commercial use in the United Kingdom (UK) to produce aggregate from industrial waste for use in concrete block manufacturing (CIWM, 2014). In essence, ACT involves a chemical reaction with water and calcium-based minerals in the waste and added carbon dioxide (CO<sub>2</sub>). The carbonate-based reaction products can cause rapid hardening of the waste, as cementation between grains forms agglomerations or monolithic materials.

In nature, carbonation is caused by the reaction between alkaline materials and atmospheric CO<sub>2</sub>, however, due to the low CO<sub>2</sub> concentration in the atmosphere, carbonation generally proceeds slowly. ACT uses a higher concentration of CO<sub>2</sub> to complete this same reaction within hours (Costa et al., 2007; Huijgen and Comans, 2005), or minutes when applied at scale. Water is added in the ACT process to form a thin aqueous film around the particles of the material being carbonated. The water layer reacts with the calcium phases in the material to form calcium hydroxide and water. Carbon dioxide injected into the mixture then reacts with the aqueous film, forming carbonic acid. Calcium ions from the calcium hydroxide react with carbonate ions of the carbonic acid to form calcium carbonate. To produce lightweight aggregates, the process is performed via a pelleting process such that aggregates are formed with concentric layers of carbonate with a “hard outer shell”. The carbonation process is exothermic, releasing heat as well as free water (Fernández et al., 2004; Arandigoyen et al., 2006; Domingo et al., 2006).

With respect to waste management practices, the main advantages of the ACT process when applied to waste materials is that: 1) it can produce a useful lightweight aggregate from the waste material, 2) it can be used for sequestration of CO<sub>2</sub>, and, 3) it can provide stabilization of some contaminants within a waste material (Fernández et al., 2004). Depending on the chemical composition of the waste material, binders such as cement may be added to promote the carbonation process and/or provide enhanced stabilization.

Waste materials such as cement kiln dust offer significant potential for manufacturing of sustainable aggregates due to its high calcium oxide (CaO) and potential to develop a stronger, more durable aggregate than that currently being developed from other industrial wastes. An additional advantage is the sequestration of CO<sub>2</sub> into a waste stream, resulting in a process that has a carbon ‘footprint’ much lower than sintered, kiln-fired or quarried and transported natural stone (see Table 1).

Global cement production in 2014 totaled 4.3 billion metric tonnes, with 82 million tonnes produced in the United States alone (CEMBUREAU, 2016). Cement Kiln Dust (CKD) is an

1 alkali-rich waste derived from cement manufacture which is normally sent to landfill if not used  
2 for other beneficial reuse products. The last decade has seen significant changes in the  
3 management of CKD, thus reducing the amount disposed to landfill (Adaska and Taubert,  
4 2008). In the US, approximately 1 million tonnes of CKD is produced (14kg for every tonne of  
5 cement clinker), with 85% of this being landfilled (PCA, 2011). The US cement industry has  
6 agreed to reduce the amount of CKD landfilled by 60%, while also curbing CO<sub>2</sub> emissions by  
7 10%, compared with 1990 levels (PCA, 2011). Amongst the largest cement producers, there is  
8 an overall drive towards resource and energy efficiency through the Cement Sustainability  
9 Initiative (CSI, 2016). Therefore, technologies that can make use of the gaseous and solid  
10 wastes from cement manufacture can potentially make a valuable contribution to achieving  
11 these goals. In this respect, accelerated carbonation has been demonstrated as a commercially  
12 viable means of recycling calcium-rich solid waste streams (such as CKD) as new construction  
13 products, whilst permanently sequestering carbon dioxide (Carbon8, 2016).  
14  
15  
16  
17  
18  
19  
20

21 Throughout the world, the requirement of aggregates for construction purposes (i.e. roadways,  
22 concrete, asphalt, etc.) is increasing. Through 2017, global consumption of aggregates is  
23 forecast to expand by 5.8% to 53.2 billion metric tons (Freedonia Group, 2013). In the United  
24 States alone, demand rose from 809 million in 2011 to 931 million tonnes in 2015 (USGS,  
25 2015). Unfortunately, in many geographical areas, aggregate supply is limited, while in  
26 developed countries, environmental permitting of mineral workings is becoming increasingly  
27 difficult. Sustainable aggregate manufacturing via ACT is one potential solution to these  
28 challenges. New technologies which are able to divert waste from landfills into carbon negative  
29 manufactured aggregates help reduce the reliance on natural resources and contribute to a  
30 circular economy.  
31  
32  
33  
34  
35  
36  
37

38 The objective of this paper is to investigate CKD as a waste-based feed-stock for the  
39 manufacture of a lightweight carbonated aggregate. No other binders or cement, were added  
40 during the ACT process. The aggregate produced will be examined for its physical and chemical  
41 properties for suitability for engineering applications, such as concrete aggregate, roadway  
42 aggregate, drainage material, or reactive permeable barriers. However, the potential end-use of  
43 the manufactured aggregate will depend on the aggregate's particle size distribution, density,  
44 strength, durability and environmental performance. The following outlines the methods used to  
45 characterize the raw CKD waste and the resulting ACT aggregate produced. Based on the test  
46 results from these characterization techniques, potential beneficial re-use applications in  
47 construction or environmental applications are then discussed.  
48  
49  
50  
51  
52  
53  
54

## 55 **2. Experimental Materials and Methods**

### 56 **2.1 Cement Kiln Dust**

57 The CKD utilized in this research was sampled from a Lafarge cement plant in Brookfield (Nova  
58 Scotia, Canada), in August 2014.  
59  
60  
61  
62  
63  
64  
65

1  
2 To gain some understanding of the chemical composition of the CKD material used in this  
3 study, two randomly selected samples (nominally 100 g of CKD-1 and CKD-2) were submitted  
4 to SGS Mineral Services Geochemical (Lakefield, Ontario, Canada) for x-ray fluorescence  
5 (XRF) analyses. Major element and rare earth oxides, and loss on ignition (LOI) were  
6 determined using a borate fusion method. Sample preparation involved taking a nominal 0.5 g  
7 of sample and forming a homogeneous glass disk by the fusion of the sample and a lithium  
8 tetraborate/lithium metaborate mixture. The LOI was determined separately and gravimetrically  
9 at 1000 °C. Disks were analyzed by wavelength dispersion fluorescence (WD-XRF). The test is  
10 accredited by the Standards Council of Canada, through the laboratory to which the samples  
11 were submitted.  
12  
13  
14  
15  
16  
17

18 As with the XRF analysis, two random samples (nominally 100g of CKD-3 and CKD-4) were  
19 submitted to Dalhousie University's Mineral Engineering Research Centre for total elemental  
20 analysis. Sample preparation involved oven-drying the samples at 60°C for 24hr, and then  
21 grinding using a mortar and pestle to less than 40 µm. Approximately 2.5g of the sample was  
22 then mixed with 5ml of nitric acid (HNO<sub>3</sub>), 5ml of hydrofluoric acid (HF) and 2 ml of chloric acid  
23 (HClO<sub>3</sub>), and heated for 12 hours by gradually raising the initial temperature of 25°C to a final  
24 temperature of 205°C. When finished, 5ml of hydrochloric acid (HCl) was added to digest the  
25 sample for 15 minutes at 120°C followed by the addition of 15ml of deionized water for 15  
26 minutes at 120°C. The digested sample was then diluted and elements analysed by inductively  
27 coupled plasma optical emission spectrometry (ICP-OES) using a Varian CCD simultaneous  
28 ICP-OES device.  
29  
30  
31  
32  
33  
34  
35  
36

37 Tables 2 and 3 show the results of the XRF and elemental analyses, respectively, for the CKD.  
38 The majority of the CKD consists of calcium, iron, silica, aluminum, magnesium and potassium  
39 oxides. Of particular note is the 42% CaO content. The high loss on ignition (LOI) for this  
40 sample indicates that the CKD has relatively low amounts of reactive free lime (Bhatty et al.,  
41 1996; Asha and Maria, 2006; Mackie et al., 2010). The approximately 10 percent of oxides  
42 unaccounted for are likely to be sulfur oxides (not measured by the method employed), as  
43 suggested by results in Table 3.  
44  
45  
46  
47  
48

## 49 **2.2 Pelletising Process Used To Produce The ACT Aggregates**

50 The moisture content, premixing time and rotation speed can all affect the size and/or strength  
51 of the aggregate produced during the ACT process (Russell et al., 2001; Beruto et al., 2005;  
52 Gunning, 2011). In this research, ACT aggregate particle size was controlled by the premixing  
53 time and water content. Table 4 shows the proportions of CKD and water used in the mixing  
54 process (based on previous trial and error by the authors). Batching of aggregates consisted of  
55 pre-mixing 400g (dry mass) of CKD with 130g water using a laboratory paddle mixer. During this  
56 phase of the mixing process, carbon dioxide was added for 90 seconds (60 seconds at 50 rpm  
57  
58  
59  
60  
61  
62  
63  
64  
65

1 speed mixing and 30 seconds at 120 rpm speed mixing). Subsequently, an additional 60g of  
2 CKD was added to the mixer and mixed for an additional 90 seconds at 50 rpm to produce more  
3 rounded aggregates. The mix was then placed in a rotating drum for 20 minutes at 50 rpm drum  
4 speed to make the aggregate (based on work reported by Gunning, 2011). Figure 1 shows a  
5 photo of the aggregate produced by this ACT process.  
6  
7

8  
9 Unless otherwise noted, ACT aggregates in this study were cured under laboratory temperature  
10 (20°C±2°C) and relative humidity (~25%) conditions for at least 28 days prior to being subjected  
11 to any testing. This air curing is representative of likely field curing conditions that would occur  
12 (i.e. in a silo). Figure 2 shows the resulting grain size distribution of three subsamples taken  
13 from the ACT aggregate produced from the pelleting process described above. As shown in  
14 Figure 2, and quantified in Table 5, there was very little variability in the aggregate grain size  
15 distribution produced using this process. The poorly graded sand, as determined from ASTM  
16 (2011c), had a relative density and moisture absorption properties as reported in Table 5.  
17  
18  
19  
20  
21  
22

### 23 **2.3. Aggregate Evaluation Tests**

#### 24 2.3.1 Internal Aggregate Porosity via Mercury Intrusion Porosimetry

25 Various factors such as porosity, pore size distribution and absorption can influence the  
26 durability properties of an aggregate (Richardson, 2009; Mindess et al., 2003). The ability of the  
27 pores in the aggregate to redistribute moisture during freeze/thaw or wet/dry events relate to  
28 many factors, but internal pore size distribution plays an important role. As discussed by  
29 Richardson (2009), aggregates with pore sizes ranging from 0.1 µm to 10 µm seem prone to  
30 freeze-thaw problems, as water distributed in these pore sizes have difficulty escaping during  
31 freezing events. It is suggested by Richardson (2009) that in aggregate with larger pores, water  
32 has the ability to leave the aggregate during freezing events and hence are less likely to be  
33 damaged.  
34  
35  
36  
37  
38  
39  
40

41 To assess the internal pore size of the ACT aggregate, mercury intrusion porosimetry (MIP) was  
42 used. Simms and Yanful (2004) review the concepts of MIP testing for examining internal pore  
43 sizes of soils. MIP involves forcing mercury into the pores of a moisture-free material under  
44 increasing amounts of pressure. The pressure required to push the mercury (a non-wetting  
45 fluid), into cylindrical-shaped pores with a diameter,  $d$ , is given by the Washburn equation  
46 (Washburn, 1921):  
47  
48  
49

$$50 \quad P = \frac{4T_s \cos\theta}{d} \quad [1]$$

51 Where:

52 P: absolute pressure

53  $T_s$  = surface tension

54  $\theta$  = contact angle between the mercury and the soil  
55  
56  
57  
58  
59  
60  
61  
62  
63  
64  
65

1 Prior to testing, samples were dried at a temperature of 150 °C for at least 24 hr to remove fluid  
2 from the pores. Several aggregate particles were weighed and placed in the sample holder prior  
3 to placement in the porosimeter (Poremaster 60, Quantachrome, USA). The sample cell was  
4 then filled with mercury and the pressure in the sample cell was increased incrementally and the  
5 volume of mercury intruded into the pores was recorded. Equation 1 was used in combination  
6 with these measurements by the Poremaster software to develop a relationship between  
7 intruded pore volume and pore diameter for the ACT aggregate.  
8  
9

## 10 11 12 2.3.2 Strength

### 13 2.3.2.1 Individual Particle Strength

14 To gain perspective on the strength of individual aggregate particles, a single pellet  
15 compressive strength test, specified in ASTM (2011a) for use with formed catalyst shapes, was  
16 used to determine strengths for single aggregate particles in this study. The particle strength  
17 was calculated using equation (2) as described by Arslan and Baykal (2006) and Li et al.  
18 (2000). Each aggregate diameter was measured at three different axes by Vernier caliper  
19 (precision 0.01mm) and the average diameter calculated. The single pellet strength was then  
20 measured using Wykeham Farrance loading frame and proving ring (capacity 4452 N, precision  
21 of 1N). The reported aggregate strength was calculated from the mean value of at least 10  
22 aggregate particles. Aggregates were tested at 7 days, 14 days and 28 days of air curing.  
23  
24  
25  
26  
27  
28  
29

$$30 \quad S = (2.8 P_c) / (\pi D^2) \quad [2]$$

31 where

32 S : the aggregate computed compressive strength (MPa)

33 P<sub>c</sub> : the failure load (MN)

34 D : the average aggregate diameter (m)

### 35 36 37 38 39 40 41 2.3.2.2 Particle Assemblage Shear Resistance via Drained Triaxial Testing

42 Any application in which an aggregate will be subjected to shear stresses (i.e. roadways,  
43 drainage on slopes, etc) will require knowledge of the drained internal angle of friction,  $\phi'$ , of the  
44 material. To estimate  $\phi'$ , consolidated isotropic drained (CID) triaxial testing was performed on  
45 the ACT aggregate assemblage under a relatively loose compaction state (i.e. a conservative  
46 approach) to establish its shear resistance under confining stress. To meet ASTM (2011b)  
47 requirements for particle size, the material described in Figure 2 was passed through a 4.75 mm  
48 sieve prior to testing. Sample preparation involved placing a sample membrane on the split  
49 mold and filling the mold and membrane partially with de-aired water. The ACT aggregates  
50 were then placed in equally spaced layers in the split mold, by allow the aggregate to free fall  
51 through the water. After the placement of a layer of ACT aggregate, light tamping of the  
52 aggregate was performed 10 times in a circular pattern using a wooden rod (49 g, 3 cm end  
53  
54  
55  
56  
57  
58  
59  
60  
61  
62  
63  
64  
65



1 diameter) dropped from a height of 5 cm. This was repeated for each of the 6 layers such that  
2 the total compaction energy was 1.3 KJ/m<sup>3</sup>. The final specimen diameter was 70 mm and the  
3 height 150 mm.  
4  
5

6 Triaxial testing used an effective confining pressure of 35 kPa followed by a saturation stage  
7 (ASTM, 2011b). After saturation was completed, the drainage lines were opened and the  
8 samples were then consolidated under the desired effective confining pressure (i.e. 100 kPa,  
9 150 kPa, 200 kPa or 250 kPa). Consolidation was deemed to be complete when sample volume  
10 change, as measured using a S-500 Triaxial/Permeability panel manufactured by Durham  
11 GeoSlope indicator (USA), ceased. Axial loading of the sample then began at a strain-controlled  
12 rate of 2 mm/min. This strain rate met ASTM (2011b) requirements for drainage during shear.  
13 Failure of the sample was either taken as the maximum value of the major principal stress,  $\sigma_1$ ,  
14 or at 15% axial strain if maximum value was not reached. Axial displacement of the specimen  
15 during testing was measured with a linear variable differential transformer (LVDT) (0.01 – 10.00  
16 mm range; MPE, United Kingdom) while axial load on the sample was measured with a 1 kg  
17 capacity load cell. LVDT and load cell measurements were recorded using a GDS data  
18 acquisition system and GDS software (GDS Instruments, UK). After the completion of the  
19 triaxial test, the specimen was air-dried and the physical appearance of the aggregate visually  
20 observed.  
21  
22  
23  
24  
25  
26  
27  
28  
29

30 Failure stresses from triaxial tests were plotted in p'-q' space. The definition of p' and q' are as  
31 previously described by Lambe and Whitman (1969):  
32  
33  
34

$$35 \quad p' = \frac{\sigma'_{1f} + \sigma'_{3f}}{2} \quad [3]$$

$$36 \quad q' = \frac{\sigma'_{1f} - \sigma'_{3f}}{2} \quad [4]$$

37 where:

38  $\sigma'_{1f}$  = maximum effective major principal stress at failure

39  $\sigma'_{3f}$  = maximum effective minor principal stress at failure

40  $\sigma'_{1f} - \sigma'_{3f}$  = effective deviator stress at failure  
41  
42  
43  
44  
45  
46  
47  
48

### 49 2.3.3 Durability

#### 50 2.3.3.1 Particle Breakage Evaluation

51 Natural carbonate sands have shown the propensity to be susceptible to particle breakage  
52 under high compression stresses (e.g. Altuhafi and Coop, 2011). Similar behaviour may be  
53 anticipated by the carbonated aggregates presented in this research. Researchers have used  
54 various types of tests to evaluate the particle breakage of aggregate assemblages (e.g. Lee and  
55 Farhoomand, 1967; Valsangkar and Holm, 1999), but testing usually involves some form of  
56 compression or shear test on the sample and monitoring changes in particle size before and  
57  
58  
59  
60  
61  
62  
63  
64  
65

1 after testing. In this research, the change in grain size of the ACT aggregate after isotropic  
2 compression in a triaxial cell was used to evaluate particle breakage (see Lee and Farhoomand,  
3 1967). Although not a standard method, it has been used by other researchers (e.g. Hardin,  
4 1985) to demonstrate particle breakage of aggregates. Similar to the triaxial testing sample  
5 preparation mentioned previously, the material shown in Figure 2 was passed through a 4.75  
6 mm sieve prior to testing, compacted in a split mold and subjected to saturation under an  
7 effective confining pressure of 35 kPa. The sample was then subjected to consolidation under  
8 an effective confining pressure of 300 kPa (a mid-range stress level that would represent a  
9 typical upper bound stress for construction applications). The grain size curves of the aggregate  
10 were compared before and after the triaxial consolidation to assess any particle breakage that  
11 may have occurred.  
12  
13  
14  
15  
16  
17

### 18 2.3.3.2 Wet/Dry Cycling

19 The slake durability test is useful in determining the durability of rocks or weak aggregate under  
20 wetting and drying conditions (ASTM, 2008). The testing in this research involved placing a  
21 known dry weight of the ACT aggregates (400 g) into the drum of the apparatus. The drum  
22 consists of a mesh with a nominal aperture size of 2.3 mm, with a length of 100 mm and a  
23 diameter of 140 mm. The drum was then rotated with the water level approximately 20 mm  
24 below the drum axis. The drum was rotated at a speed of 10 rpm for a period of 10 minutes.  
25 After slaking for 10 minutes, aggregates were then dried in an oven at a temperature of 105 °C  
26 for up to 6 hrs. The mass of dried samples was weighed to obtain the mass remaining after the  
27 first cycle. The test was repeated for another cycle and the dry mass again reported. The  
28 percent of sample remaining after these wet-dry cycling tests was then recorded.  
29  
30  
31  
32  
33  
34  
35  
36  
37

### 38 2.3.3.3 Freeze Thaw

39 As noted by Edwards (2006), it is important to understand any changes in aggregates as they  
40 undergo freeze thaw. Disintegration of aggregates to finer grain size after freeze thaw could  
41 cause unwanted settlement or instability in roadway applications or clogging in drainage  
42 applications. Past studies have shown that resistance to freeze/thaw cycling can be influenced  
43 by the aggregate moisture content and strength (Edwards, 2006). In this study, the initial  
44 aggregate grainsize (400 g sample) as shown in Figure 2 was initially soaked in water for 4  
45 hours. After soaking, the aggregates were allowed to surface dry for approximately 15 minutes.  
46 The test aggregate samples were then subjected to 10 or 20 freeze-thaw cycles which included  
47 freezing to  $-17.5 \pm 2.5^{\circ}\text{C}$  for 24 hours and then thawing in a water bath at room temperature ( $\sim$   
48  $20^{\circ}\text{C} \pm 2^{\circ}\text{C}$ ) for 4 hours (see BSI, 2002a). The temperatures chosen reflect the British Standard  
49 BS EN 130055-1 (BSI, 2002a). After the end of the freeze-thaw cycles, the samples were  
50 subjected to grain size analysis to compare particle size distribution before and after freeze-  
51 thaw cycling. In addition, MIP testing as described in section 2.3.1 was performed on the  
52  
53  
54  
55  
56  
57  
58  
59  
60  
61  
62  
63  
64  
65

1 aggregate before and after freeze thaw to examine the potential for changes in pore size  
2 distribution after freeze thaw.  
3  
4  
5

#### 6 2.3.4 ACT Aggregate Geo-environmental Properties: Leachate Testing, Single Point, Batch 7 Sorption Testing and Hydraulic Conductivity 8 9

10 Cement kiln dust is normally landfilled due to its high pH, particle size and soluble heavy metals.  
11 Thus, the potential for the ACT aggregate to be used in practice will ultimately rely on the  
12 management of risk, including leaching of any contaminants (i.e. metals) from the aggregate. To  
13 assess metals leaching, a modification of the British Standard for evaluating wastes was used  
14 (BSI, 2002b). The procedure involved taking a 20 g sample of the aggregate (not crushed to  
15 reflect actual conditions) and combined with 200 g of de-ionised water in glass bottles. The  
16 bottles were then rotated for 24 hours after which the resultant leachate was filtered through a  
17 0.45 um filter. Samples were then subjected to metal analyses with inductively coupled plasma  
18 optical emission spectrometry (ICP-OES) using a Varian CCD simultaneous ICP-OES device.  
19  
20  
21  
22  
23  
24  
25

26 If the aggregate were to be used in any type of permeable barrier application for metal retention  
27 (i.e. storm water, acid drainage, wastewater etc.), a knowledge of the capacity of the aggregate  
28 to sorb metals is required. To establish estimates of sorption properties of the ACT aggregate  
29 for potential metal removal applications, a modified version of ASTM C1733 was used. Since  
30 the goal of the testing was to quickly examine sorption properties for a range of different metal  
31 solutions, the modification involved a single point batch sorption test which was adopted with  
32 separate 500µg/l solutions of chromium, zinc, cadmium, arsenic, lead and copper, combined  
33 with 10g (dry weight) of the ACT aggregates. Each 200 ml solution and ACT aggregate was  
34 placed on a rotating shaker table for 48hr at 100 rpm. After 48hr, the samples were vacuum  
35 filtered through a fritted-glass crucible fitted with a filter paper to retain the precipitate. After  
36 filtering, 2-3 drops of HNO<sub>3</sub> acid was added to each of the filtered solutions and the samples  
37 were then submitted to Dalhousie University Clean Water Laboratory Centre for analysis. Each  
38 metal was quantified by Inductively Coupled Plasma Mass Spectrometry (ICP-MS) analysis.  
39  
40  
41  
42  
43  
44  
45  
46

47 The potential to use the aggregate for drainage in roadway applications, septic system  
48 drainage, permeable reactive barriers, etc. requires an estimate of the hydraulic conductivity.  
49 The hydraulic conductivity of the aggregate was established via the constant head test method  
50 (ASTM, 2006). Hydraulic conductivity tests used ACT-derived CKD aggregates air-cured for 7  
51 days. Samples were loosely tamped into the constant head permeameters using an  
52 approximate energy level of 7900 J/m<sup>3</sup>.  
53  
54  
55  
56  
57

### 58 **3. Test Results**

#### 59 3.1 Internal Aggregate Porosity via Mercury Intrusion Porosimetry 60 61 62 63 64 65

1 Figure 3 shows the pore size distribution of the CKD aggregate, as measured by MIP. It can be  
2 seen that the majority of pores range from approximately 0.01  $\mu\text{m}$  to slightly less than 1  $\mu\text{m}$ . As  
3 noted by Richardson (2009), this pore size distribution may be an indication of freeze thaw  
4 susceptibility, although other factors such as particle size, particle strength, pore length,  
5 mineralogy, absorption, and specific gravity can also have an influence. Also shown on Figure 3  
6 is the pore size distribution of the aggregate after 20 cycles of freeze thaw. It appears there was  
7 very little change in the pore structure of the aggregate after 20 cycles of freeze thaw. Rupturing  
8 of the pores due to freeze thaw damage would not be detected by this test method as this would  
9 result in particle breakage of the aggregate. Hence any major changes in pore size that could  
10 cause rupture would only be detected visually or through changes in grain size, and is  
11 discussed further in section 3.3.3.  
12  
13  
14  
15  
16  
17

## 18 3.2 Strength

### 19 3.2.1 Individual Particle Strength

20 As shown in Figure 4, average individual aggregate strengths reached 0.8 MPa after 7 days of  
21 curing, 1.1 MPa after 14 days of curing and 1.2 MPa after 28 days of curing. The variability of  
22 the test results are presented in Figure 4 via error bars, showing one standard deviation from  
23 the mean. This strength gain is due to carbonation/hydration continuing over 28 days. It should  
24 be noted that the strengths reported in Figure 4 are comparable to commercially available  
25 sintered light-weight aggregates (e.g. Lytag sintered aggregate strength: 0.4 MPa; see Gunning,  
26 2011).  
27  
28  
29  
30  
31

### 32 3.2.2 Particle Assemblage Shear Resistance via Drained Triaxial Testing

33 Isotropic drained triaxial test results are shown on Figure 5. As would be expected for a re-  
34 compacted soil (dry unit weights for the ACT samples tested ranged from 11.5  $\text{kN/m}^3$  to 11.7  
35  $\text{kN/m}^3$ ), deviator stresses at failure exhibited slow, sustained increases to the maximum axial  
36 stress. The subsequent stress paths of the triaxial tests are plotted in  $p'$ - $q'$  space (Figure 6). The  
37 results of the stress conditions at failure show a linear trend as the confining pressures  
38 increased. When fitting a regression line through the origin, the drained friction angle of the  
39 aggregate is established as  $39^\circ$ . It is interesting to note that the shear strength envelope  
40 remains linear at the higher confining pressures which suggests that there is no significant  
41 breakage of the aggregate at these confining stresses resulting in a degradation of strength. No  
42 particle breakage was observed in post-test inspection of the aggregate.  
43  
44  
45  
46  
47  
48  
49  
50  
51

## 52 3.3 Durability

### 53 3.3.1 Particle Breakage Evaluation

54 The particle size distributions for the ACT aggregate before and after isotropic consolidation in  
55 the triaxial cell at 300 kPa are shown in Figure 7. As can be seen from the figure, very little, if  
56 any, changes in the grain size of the sample occurred after the application of the 300 kPa  
57 effective stress on the sample. As well, no visual deterioration of the aggregate was observed.  
58  
59  
60  
61  
62  
63  
64  
65

1 The confining pressure of 300 kPa equates to burial at a depth of approximately 25 m depth  
2 (unit weight of 12 kN/m<sup>3</sup> and without a static water table) and preliminary results suggest that  
3 damage to the aggregate would be minimal at similar effective stresses and isotropic stress  
4 conditions. It should be noted that Lee and Farhoomand (1967) showed that anisotropic loading  
5 can influence the amount of particle breakage observed.  
6  
7

### 8 9 10 3.3.2 Wet/Dry Strength Test

11 The results of the slake durability test are presented in Table 6. Similar to the limited amount of  
12 particle breakage observed after the isotropic compression of the aggregate presented in the  
13 previous section, the wet-dry cycling, as performed using the slake durability test resulted in  
14 very little change in the ACT aggregate after 2 cycles. Although this is a fairly empirical test  
15 method designed for rock materials, according to the Gamble (1971) classification, the  
16 aggregate achieved a very high durability rating.  
17  
18  
19  
20  
21  
22

### 23 3.3.3 Freeze/Thaw Cycle Tests

24 As discussed in section 2.3.3.3, two subsamples of aggregates were subjected to 10 or 20  
25 freeze thaw cycles. Grain size distributions before and after the freeze thaw cycling are shown  
26 on Figure 8. The grain size distribution before freeze thaw are presented in comparison to the  
27 range of grain size observed in Figure 2 (error bars on Figure 8). Unlike the two previous  
28 durability tests, freeze thaw cycling appeared to have an effect on the grain size of the  
29 aggregate. After 10 cycles of freeze thaw, the 2.5 mm aggregate fractions became noticeably  
30 finer, while less change at this fraction was observed at the end of the 20<sup>th</sup> freeze thaw cycle.  
31 Overall there was a general shift in the original grain size distribution curve, moving to a finer  
32 grain size. Photos of the ACT aggregate during the f/t cycling process are provided in Figure 9,  
33 and show an apparent reduction in the size of the larger aggregates, as opposed to the smaller  
34 aggregates. The breakage of the ~ 5 mm particles appeared to result from the flaking of the  
35 outer surface of the aggregate and this behavior is subject to further detailed work by the  
36 authors.  
37  
38  
39  
40  
41  
42  
43  
44  
45

### 46 3.4 ACT Aggregate Geo-environmental Properties: Leachate Testing, Single Point, Batch 47 Sorption Testing and Hydraulic Conductivity 48

49  
50 The leaching test results for the ACT aggregate are shown in Table 7. The table shows the  
51 results of triplicate analyses of the aggregate (ACT-1,2,3) compared to the average total mass  
52 of the metals reported in the CKD sample in Table 3. Results are reported both in terms of mass  
53 of metal leached per dry mass of ACT (to allow comparison to Table 3) as well as leachate  
54 concentrations. Only the metals detected in Table 3 are reported in Table 7. As can be seen  
55 from Table 7, of the metals detected in the ACT aggregate from Table 3, many of these metals  
56 did not leach from the aggregate to any appreciable level; many were below the detection limit  
57  
58  
59  
60  
61  
62  
63  
64  
65

1 of the method. Also shown in Table 7 for comparison to leachate values are groundwater  
2 standards that must be met in the province of Nova Scotia (NSE, 2013), Canada (the source of  
3 the CKD) for remediation. Ba, Cr, Sr, and Zn leaching was observed for the aggregate, but were  
4 below the groundwater guidelines provided in Table 7. As noted from Table 7 results, there was  
5 minimal leaching of the metals shown from the ACT aggregate and provides insight into the  
6 ability of the carbonation process to stabilise and solidify CKD.  
7  
8  
9

10 The single point batch tests with the heavy metal ions and the ACT aggregate allowed for a  
11 preliminary assessment of the aggregate's adsorptive properties for potential reactive barrier  
12 applications. As noted in Table 8, very good removal rates were observed for all of the heavy  
13 metals tested. The pH in the flasks ranged from 11.3 to 11.5 after 48 hours of mixing with the  
14 ACT aggregate and metal solutions. The alkaline nature of the ACT aggregate likely contributed  
15 to the high removal rates as well as the high absorption ability of the aggregate (i.e. internal  
16 porosity).  
17  
18  
19  
20  
21  
22

23 The ACT derived CKD aggregate hydraulic conductivity varied little, as would be expected given  
24 the lack of grain size variability in the ACT derived CKD aggregate particle size. Measurement  
25 of the hydraulic conductivity on three different samples yielded hydraulic conductivities of  
26  $1.5 \times 10^{-4}$  m/s,  $1.5 \times 10^{-4}$  m/s, and  $1.4 \times 10^{-4}$  m/s. The dry density of the tested samples was 1190  
27 kg/m<sup>3</sup>.  
28  
29  
30

#### 31 **4 Discussion**

32 The use of waste to generate new construction materials that are fit for purpose offers  
33 significant sustainability gains. A 'cold' process, such as used here, will have low energy  
34 requirements and result in an attractive carbon 'footprint'. Other benefits include: 1) a route for  
35 the valorisation of waste that would otherwise be disposed of in landfill, 2) a feedstock that can  
36 substitute for virgin stone and, 3) carbon dioxide, otherwise released to the atmosphere, is  
37 permanently sequestered into the aggregate as a carbonate cement. The objective of this paper  
38 was to explore the carbonation potential of CKD to produce an aggregate that has physical and  
39 chemical properties that enable beneficial re-use in, for example, concrete, roadway  
40 engineering, drainage materials or reactive permeable barriers.  
41  
42  
43  
44  
45  
46  
47  
48

49 One of the attractive properties resulting from cementation by carbonation is the low density  
50 compared to most natural aggregates (a bulk density of 1100 kg/m<sup>3</sup> compared to >2000 kg/m<sup>3</sup>,  
51 respectively). As aggregates produced in the geosphere are normally formed at great depth and  
52 at elevated temperature, they tend to be dense in nature. However, when using ACT to  
53 carbonate waste at or near normal atmospheric temperatures and pressures, the density of the  
54 carbonate cemented product is technically "lightweight", although not as lightweight as some  
55 sintered or bloated commercially manufactured aggregates (see Table 9 for a comparison).  
56 Thus, the CKD-based aggregate is lighter than natural aggregate, but denser (both particle and  
57  
58  
59  
60  
61  
62  
63  
64  
65

1 bulk) than expanded clay, shale, and glass aggregates and sintered fly ash. The manufactured  
2 aggregates given in Table 9 (with the exception of the C8A aggregate) are produced using high  
3 energy intensive processes, primarily extreme heating in their production, and have a high  
4 'carbon footprints'.  
5

6  
7  
8 The individual particle strength of the CKD aggregate is within the range of the other aggregates  
9 shown in Table 9, and in recent work by the authors using a modified processing method of  
10 CKD aggregate, individual particle strengths greater than 4MPa have been achieved. This  
11 suggests improved durability properties with respect to freeze thaw may be realised.  
12  
13

14  
15 In comparison with Nova Scotian quarried aggregate, with particle strengths ranging from 25  
16 MPa to 300 MPa, the particle strength of carbonated CKD aggregate is low, and its freeze thaw  
17 resistance, particle breakage (under wet/dry), compression and shear conditions is not  
18 surprisingly inferior. However it would be suitable as fill material for roadway construction given  
19 its adequate performance in wet/dry testing and triaxial compression and shear.  
20  
21  
22

23  
24 In the province of Nova Scotia, the use of "borrow" material for fill is limited little by specification  
25 (see NSTIR, 2014) and more by its engineering performance properties and environmental  
26 characteristics (NSE, 2013) in determining that an aggregate is "fit for purpose" in roadway  
27 construction applications. Given its good drainage and lightweight characteristics, the aggregate  
28 would be beneficial as backfill for retaining structures. The low bulk density relative to natural  
29 aggregates and adequate internal angle of friction would serve to reduce loads on the retaining  
30 wall, resulting in more economical designs (i.e. smaller walls).  
31  
32  
33  
34

35  
36 Further applications such as in permeable reactive barriers where the sorption of metals is  
37 important could be another application for investigation. For the specific metals examined here,  
38 over 90% were removed from solution in single point sorption tests on exposure to the CKD  
39 aggregate. Metals removal is likely due to the internal porosity available within the aggregate as  
40 well as the alkaline aggregate surface which promotes metal precipitation; as such the potential  
41 interaction of the aggregate and ground water passing through a permeable barrier would have  
42 to be assessed using long term testing/modelling studies.  
43  
44  
45  
46  
47

48  
49 It has been the authors' experience that the beneficial properties of manufactured aggregates  
50 are key to market development. When the technical advantages are combined with government  
51 carbon offset incentives (being discussed more frequently in Canada) and the drive to a circular  
52 economy (ECCC, 2016), low carbon solutions become attractive to regulators, specifiers and  
53 construction materials users alike.  
54  
55  
56  
57  
58  
59  
60  
61  
62  
63  
64  
65

## 5 Summary and Conclusions

To assess the geotechnical and geo-environmental properties of carbonated aggregate made from CKD, several performance tests were applied to gauge potential re-use options. The sand product was shown to have a mature individual aggregate strength of more than 1 MPa, and upon compaction a friction angle of 39° when subjected to drained triaxial testing, under confining pressures ranging from 100 kPa to 250 kPa. The aggregate displayed a very high durability to wet-dry cycling using the slake durability test and no noticeable changes in grain size when subjected to an isotropic confining compression test. Freeze thaw cycling at -17.5 ±2.5°C for 20 cycles showed a reduction in grain size that warrants further investigation, and future improvement. One-point batch adsorption showed that the ACT aggregate removed 90% of the selected heavy metals from prepared solutions, indicating potential for geo-environmental applications such as permeable reactive barriers. The resulting grain size and hydraulic conductivity of the aggregate suggest it is a reasonably permeable material that may be used in drainage or permeable reactive barrier applications.

Future studies on the aggregate will focus more on its durability to determine its performance under environmental loading and on optimizing its particle size distribution and curing to improve its durability and performance for use in real-world applications.

### Acknowledgements

The authors would like to acknowledge Carbon8 Systems for their permission to utilize the ACT aggregate process to produce the CKD aggregates. Funding for the research was provided by NSERC CREATE and Discovery grant programs.

### References

- Adaska S W and Taubert H D (2008) Beneficial uses of Cement Kiln Dust. *Presented at 2008 IEEE/PCA 50th Cement Industry Technical Conference*. Miami, Florida, USA, pp. 210-228.
- Altuhafi, F N and Coop, M R (2011) Changes to particle characteristics associated with the compression of sands. *Geotechnique* **61(6)**: 459–471.
- Arandigoyen M, Bicer-Simsir B, Alvarez J I and Lange D A (2006) Variation of microstructure with carbonation in lime and blended pastes. *Journal of Applied Surface Science* **252(20)**: 7562-7571.
- Arslan H and Baykal G (2006) Analyzing the crushing of granular materials by sound analysis technique. *Journal of Testing and Evaluation* **34(6)**: 1-7.
- Asha S and Maria C S (2006) Development of criteria for the utilization of cement kiln dust (CKD) in highway infrastructures. Purdue University, West Lafayette, Indiana, USA, Report FHWA/IN/JTRP-2005/10.
- ASTM (2006) D2434-68: Standard Test Method for Permeability of Granular Soils (Constant Head). ASTM International, West Conshohocken, PA, USA (withdrawn).



1 ASTM (2008) D4644-08: Standard Test Method for Slake Durability of Shales and Similar Weak  
2 Rocks. ASTM International, West Conshohocken, PA, USA.

3 ASTM (2011a) D4179-11: Standard Test Method for Single Pellet Crush Strength of Formed  
4 Catalysts and Catalyst Carriers. ASTM International, West Conshohocken, PA, USA.

5  
6 ASTM (2011b) D7181: Standard Test Method for Consolidated Drained Triaxial Compression  
7 Test for Soils. ASTM International, West Conshohocken, PA, USA.

8  
9 ASTM (2011c) D2487: Standard Test Method for Classification of Soil For Engineering  
10 Purposes (Unified Soil Classification System, ASTM International, West Conshohocken, PA,  
11 USA.

12  
13 ASTM (2015) C128: Standard Test Method for Relative Density (Specific Gravity) and  
14 Absorption of Coarse Aggregate. ASTM International, West Conshohocken, PA, USA.

15  
16 Beruto D T, Barberis F and Botter R (2005) Calcium carbonate binding mechanisms in the  
17 setting of calcium and calcium-magnesium putty-limes. *Journal of Cultural Heritage* **6(3)**: 253-  
18 260.

19  
20 Bhatta, J I, Bhattacharja, S, Todres, H A (1996) Use of cement kiln dust in stabilizing clay soils.  
21 Portland Cement Association R&D Serial No. 2035, Portland Cement Association, Skokie,  
22 Illinois, USA.

23  
24 BSI, British Standards Institution (2002a) BS EN 13055-1:2002: Lightweight aggregates.  
25 Lightweight aggregates for concrete mortar and grout. BSI, London, UK.

26  
27 BSI, British Standards Institution (2002b) BS EN 12457-4:2002: Characterisation of waste.  
28 Leaching. Compliance test for leaching of granular waste materials and sludges. BSI, London,  
29 UK.

30  
31 BSI, British Standards Institution (2016) BS EN 12457-4:2016: Lightweight aggregates.  
32 Lightweight aggregates for concrete mortar and grout. BSI, London, UK.

33  
34 Carbon8 (2016). Company website for Carbon8 Aggregates Limited, see <http://c8a.co.uk/>  
35 (accessed March 10, 2016).

36  
37 CEMBUREAU (2016). European Cement Association (CEMBUREAU). Key facts and figures.  
38 see <http://www.cembureau.be/> (accessed March 10, 2016).

39  
40 CIWM (2014) Grondon Invests Further Millions In Carbon8 Aggregates. *Chartered Institution of*  
41 *Wastes Management*, see <http://www.ciwm.co.uk/> (accessed March 10, 2016).

42  
43 Costa I, Baciocchi R, Poletini, A, Pomi R, Hills C D and Carey P J (2007) Current status and  
44 perspectives of accelerated carbonation processes on municipal waste combustion residues.  
45 *Environmental Monitoring Assessment* **135(1)**: 55-75.

46  
47 CSI (2016) Cement Sustainability Initiative, World Business Council for Sustainable  
48 Development, see: <http://www.wbcscement.org/> (accessed March 10, 2016).

49  
50 Domingo C, Loste E, Gomez-Morales J, Garcia-Carmona J and Fraile J (2006) Calcite  
51 precipitation by a high-pressure CO<sub>2</sub> carbonation route. *The Journal of Supercritical Fluids*  
52 **36(3)**: 202-215.

53  
54 ECCC (2016) Canada's second biennial report on climate change. Environment and Climate  
55 Change Canada.

- 1 Edwards L M (2006) The effect of alternate freezing and thawing on aggregate stability and  
2 aggregate size distribution of some Prince Edward Island soils. *Journal of Soil Science* **42(2)**:  
3 193-204.
- 4 Fernández B M, Simons S J R, Hills C D and Carey P J (2004) A review of accelerated  
5 carbonation technology in the treatment of cement-based materials and sequestration of CO<sub>2</sub>.  
6 *Journal of Hazardous Materials* **112(3)**: 193-205.
- 7  
8 Freedonia Group (2013). *Industry Study 3078: World Construction Aggregates*.  
9
- 10  
11 Gamble, J C (1971) *Durability-plasticity classification and shales and other argillaceous rocks*,  
12 PhD Thesis, University of Illinois, USA.
- 13  
14 Gunning P J (2011) *Accelerated Carbonation of Hazardous Wastes*. Doctoral dissertation.  
15 Greenwich University, UK.
- 16  
17 Gunning P J, Hills C D, and Carey P J (2009) Production of lightweight aggregate from  
18 industrial waste and carbon dioxide. *Waste Management* **29**:2722–2728.
- 19  
20 Hardin (1985) Crushing of soil particles. *ASCE Journal Geotechnical Engineering* **111(10)**:  
21 1177-1192
- 22  
23 Huijgen W J and Comans R N J (2005) *Carbon Dioxide Sequestration by Mineral Carbonation:*  
24 *Literature review update 2003-2004*. Energy Research Centre of the Netherlands. Report ECN-  
25 C—05-022.
- 26  
27 Lambe T W and Whitman R V (1969) *Soil Mechanics*. Wiley, New York, USA, pp. 423-455.
- 28  
29 Lee, K L and Farhoomand, I (1967) Compressibility and crushing of granular soil. *Canadian*  
30 *Geotechnical Journal* **4(1)**:68-86.
- 31  
32 Li Y, Wu D, Zhang J, Chang L, Wu D, Fang Z and Shi Y (2000) Measurement and statistics of  
33 single pellet mechanical strength of differently shaped catalysts. *Powder Technology* **113(1-**  
34 **2)**: 176-184.
- 35  
36 Lytag (2016). Company website for Lytag lightweight aggregate, see <http://www.lytag.com/>  
37 (accessed March 10, 2016).
- 38  
39 Mackie A, Boilard S, Walsh M E and Lake, C B (2010) Physicochemical characterization of  
40 cement kiln dust for potential reuse in acidic wastewater treatment. *Journal of Hazardous*  
41 *Materials* **173(1-3)**: 283-291.
- 42  
43 Mindess S, Young J F and Darwin D (2003) *Concrete*. New Jersey, Pearson Prentice Hall, pp.  
44 121-163.
- 45  
46 Nesolite (2016) Company website for Solite Lightweight Aggregate, see  
47 <http://www.nesolite.com/> (accessed on March 10, 2016).
- 48  
49 NSE, Nova Scotia Environment (2013) *Notification of Contamination Protocol*, PRO-100,  
50 Province of Nova Scotia, Canada, see:  
51 <http://www.novascotia.ca/nse/contaminatedsites/protocols.asp> (accessed August 17, 2016).
- 52  
53 NSTIR, Nova Scotia Transportation and Infrastructure Renewal (2014) Standard specification,  
54 Highway Construction and Maintenance, Province of Nova Scotia, Canada, see  
55 <https://novascotia.ca/tran/publications/standard.pdf> (accessed March 9, 2016).
- 56  
57 PCA (2011) Report on sustainable manufacturing, Portland Cement Association, see  
58 <http://www.cement.org/> (accessed March 10, 2016).
- 59  
60  
61  
62  
63  
64  
65

1 Poraver (2016) Company website for Poraver Expanded Glass, see [www.poraver.com](http://www.poraver.com)  
2 (accessed March 10, 2016).

3 Richardson D N (2009) *Quick Test for Durability Factor Estimation*. Missouri University of  
4 Science and Technology, Rolla, Missouri, USA, Report 0R09.020, pp. 24-30.

5  
6 Russell D, Basheer, P A M, Rankin G I B and Long A E (2001) Effect of relative humidity and air  
7 permeability on prediction of the rate of carbonation of concrete. *Proceedings of the Institution*  
8 *of Civil Engineers-Structures and Buildings* **146(3)**: 319-326.

9  
10 Simms, P H and Yanful, E K (2004). A discussion of the application of mercury intrusion  
11 porosimetry for the investigation of soils, including an evaluation of its use to estimate  
12 volume change in compacted clayey soils. *Geotechnique* **54(6)**: 421–426.

13  
14 USGS (2015) Mineral Commodity Summaries, United States Geological Survey, see  
15 <http://minerals.usgs.gov/minerals/pubs/commodity/> (accessed March 10, 2016).

16  
17 Valsangkar, A J and Holm, T A (1999) Mechanical Durability of Expanded Shale Lightweight  
18 Aggregate. *Geotechnical Testing Journal* **22(4)**:329–333.

19  
20 Washburn, E. W. (1921) Note on a method of determining the distribution of pore sizes in a  
21 porous material. *Proceedings National Academy of Sciences* **7**:115–116.

22  
23 Weber Saint Gobain (2016). Company website for Leca UK lightweight aggregate, see  
24 [www.leca.co.uk](http://www.leca.co.uk) (accessed March 10, 2016).

**List of Figures**

Figure 1. ACT derived CKD aggregate (photo by author)

Figure 2. Grain size distribution of ACT aggregate

Figure 3. Pore diameter of the ACT as measured by MIP (before and after 20 cycles of freeze thaw).

Figure 4. Average ACT individual aggregate strength related to curing time (error bars denote one standard deviation from the mean).

Figure 5. Stress strain curves for triaxial testing

Figure 6. Failure envelope for ACT aggregate from CID triaxial testing

Figure 7. Comparison of grain size curves before and after triaxial consolidation at an effective confining pressure of 300 kPa.

Figure 8. Results of freeze thaw cycling; comparing grain size distributions before and after 10 and 20 cycles of freeze thaw.

Figure 9. ACT aggregate photos before and after 10 and 20 cycles of freeze thaw

**List of Tables**

Table 1. Categories and examples of lightweight aggregate (modified from BS EN 13055: 2016)

Table 2. Major oxide results for the CKD used in this study.

Table 3. Elemental analysis for the CKD used in this study\*

Table 4. ACT Derived CKD Aggregate Mix Design and Pelleting Production Process

Table 5. Grain size, relative density and absorption of ACT derived CKD aggregates

Table 6. Slake durability test results

Table 7. Leaching test results on ACT aggregate

Table 8. Single point heavy metal ion batch testing.

Table 9. Comparison of Physical Properties of Various Manufactured Aggregates.



Figure 2

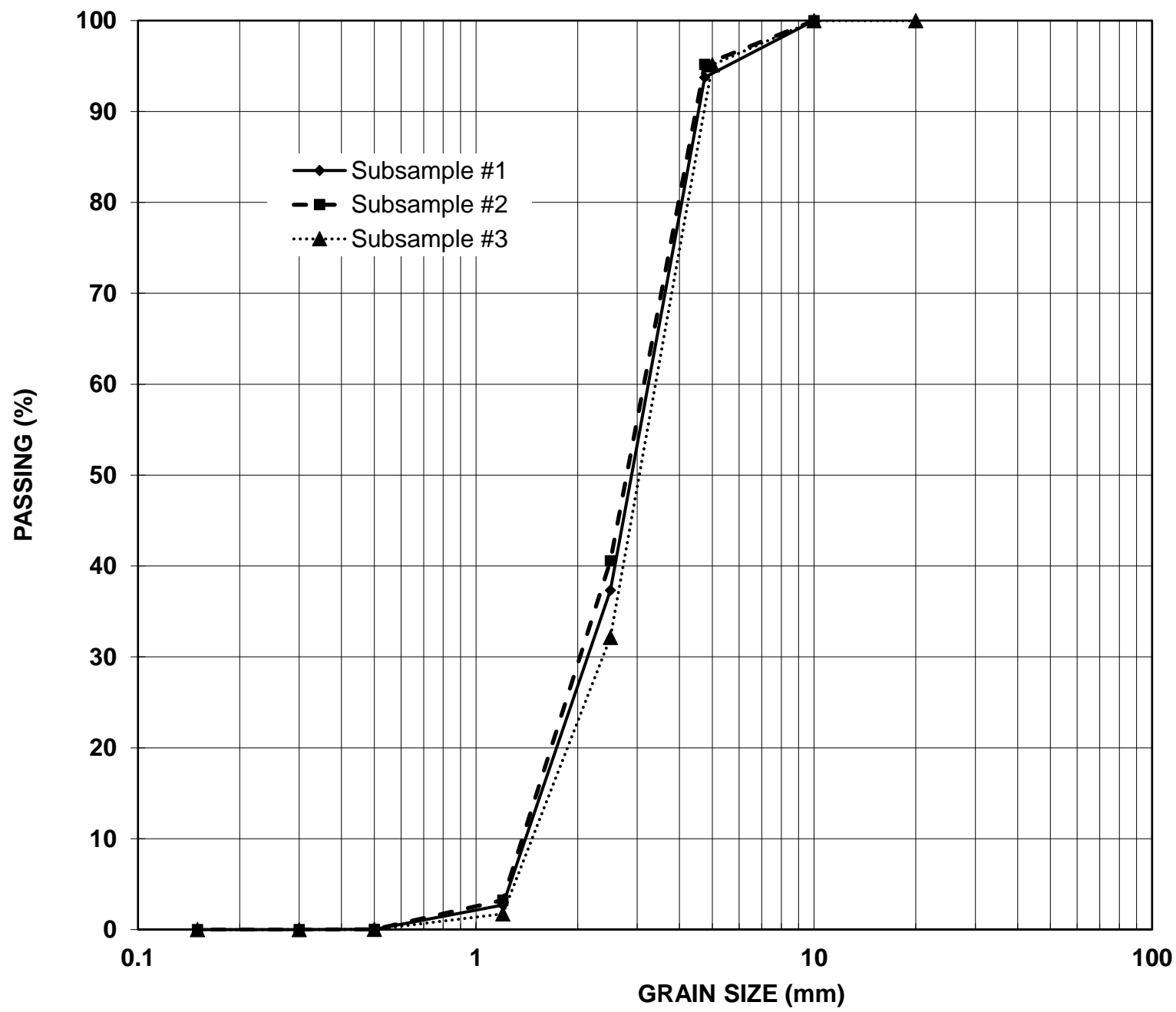


Figure 3

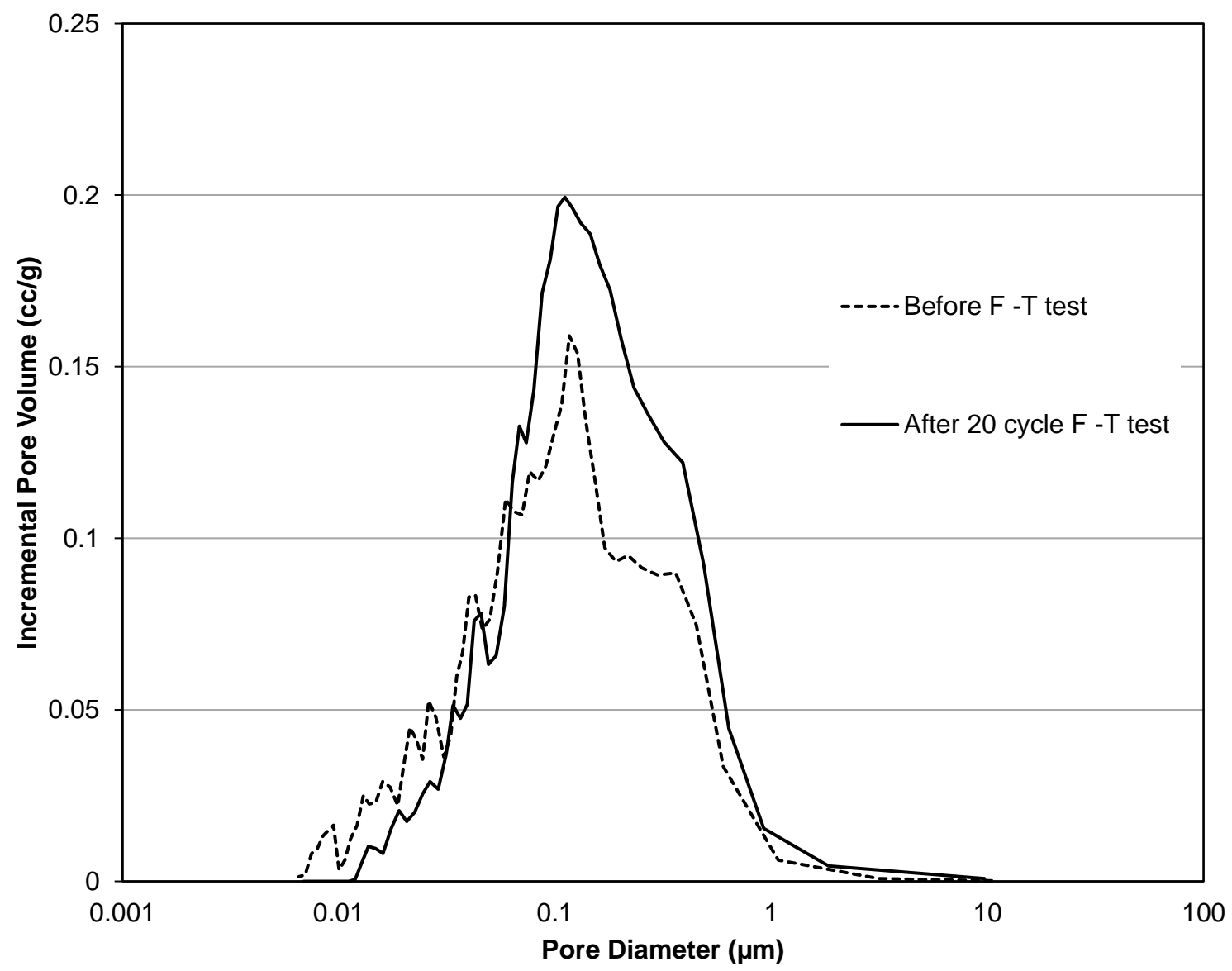




Figure 4

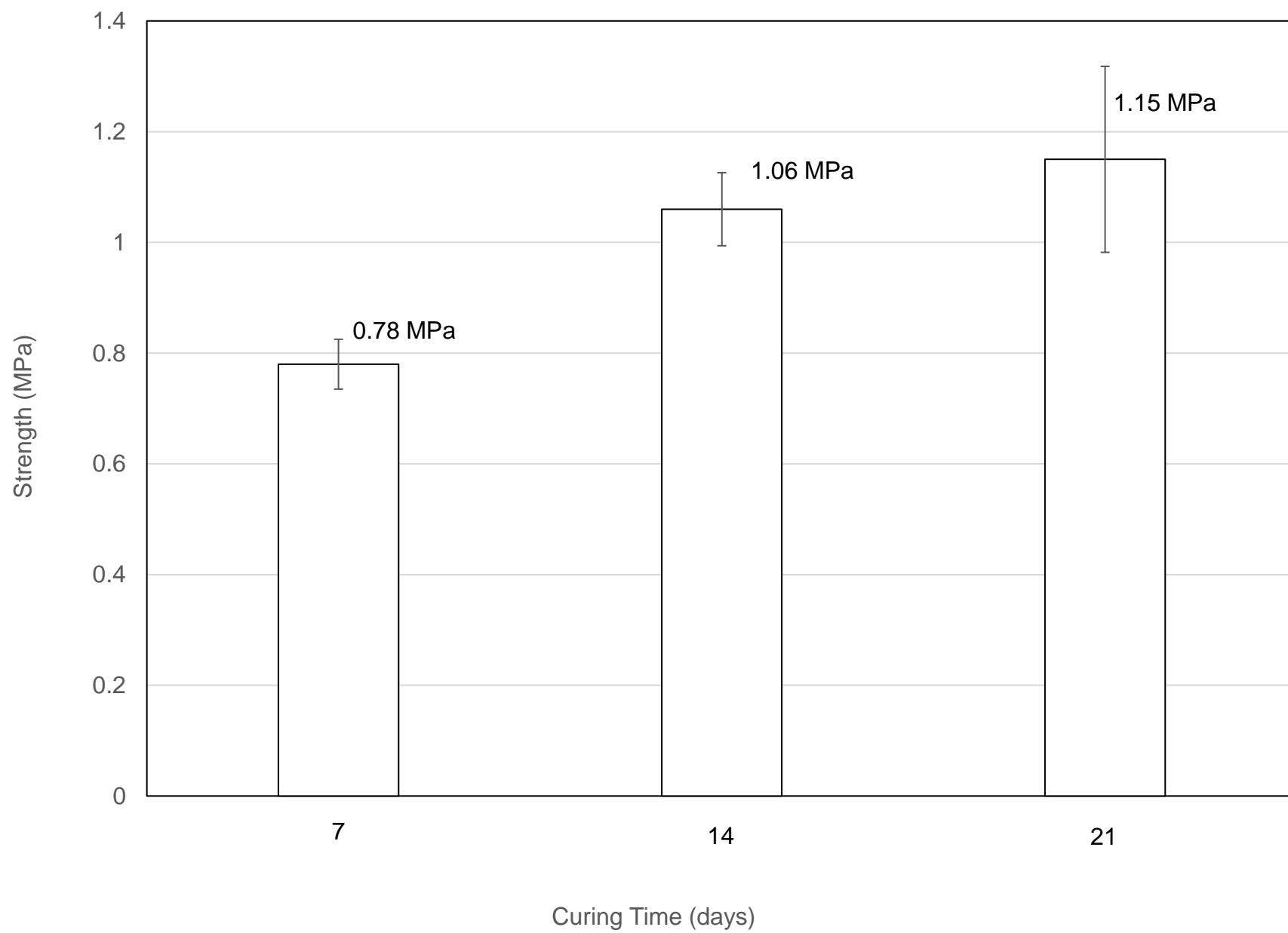


Figure 5

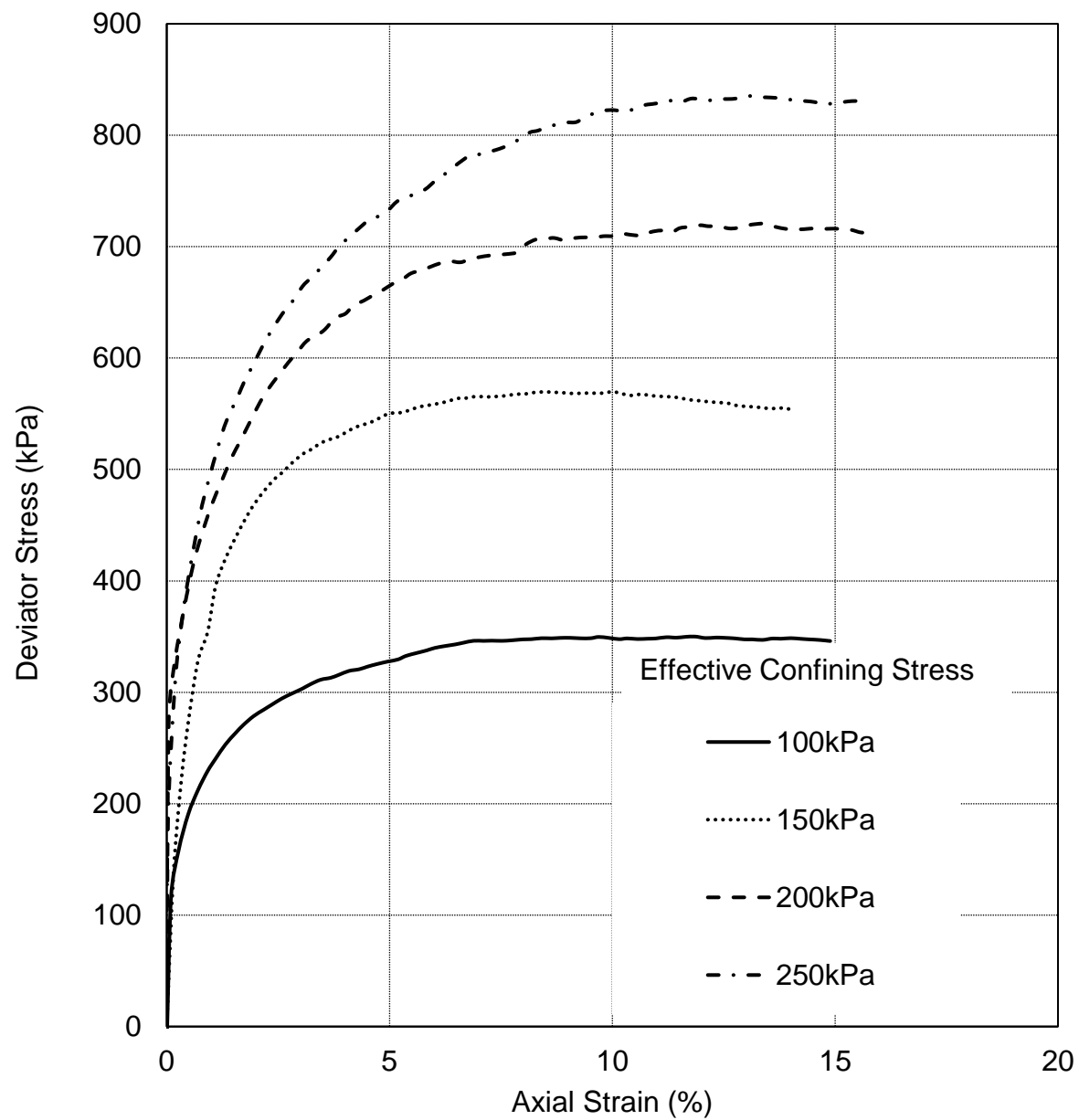


Figure 6

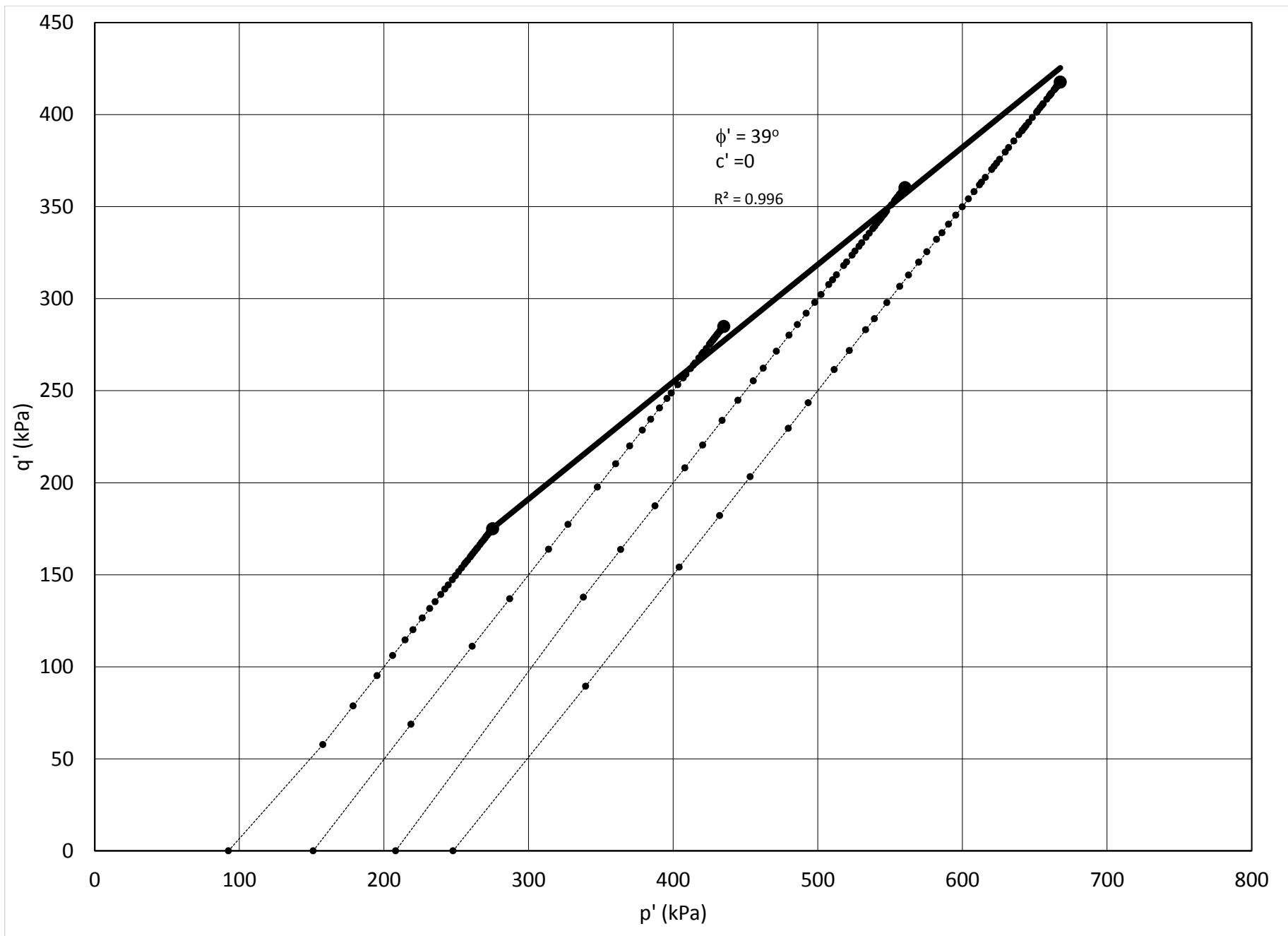


Figure 7

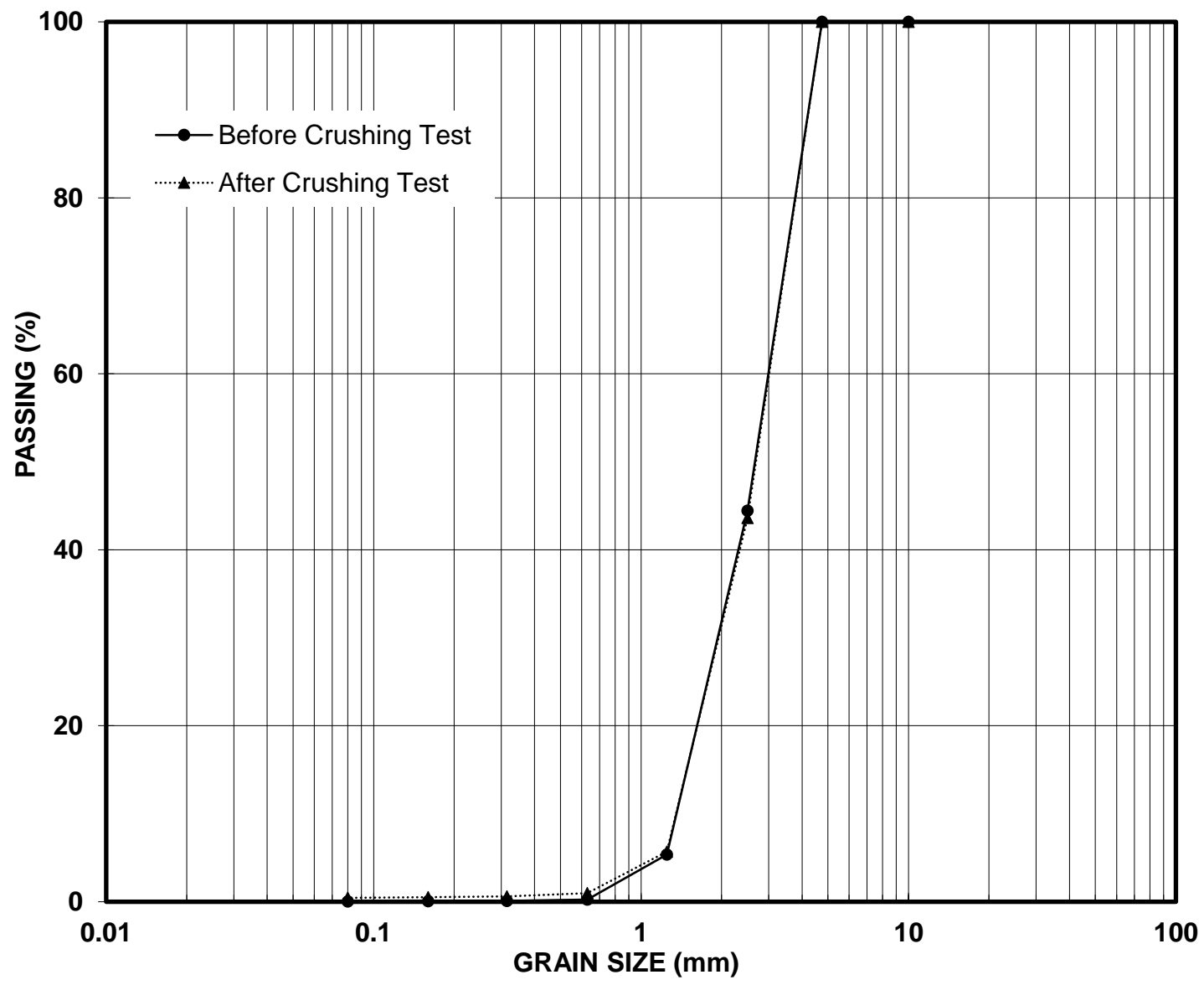


Figure 8

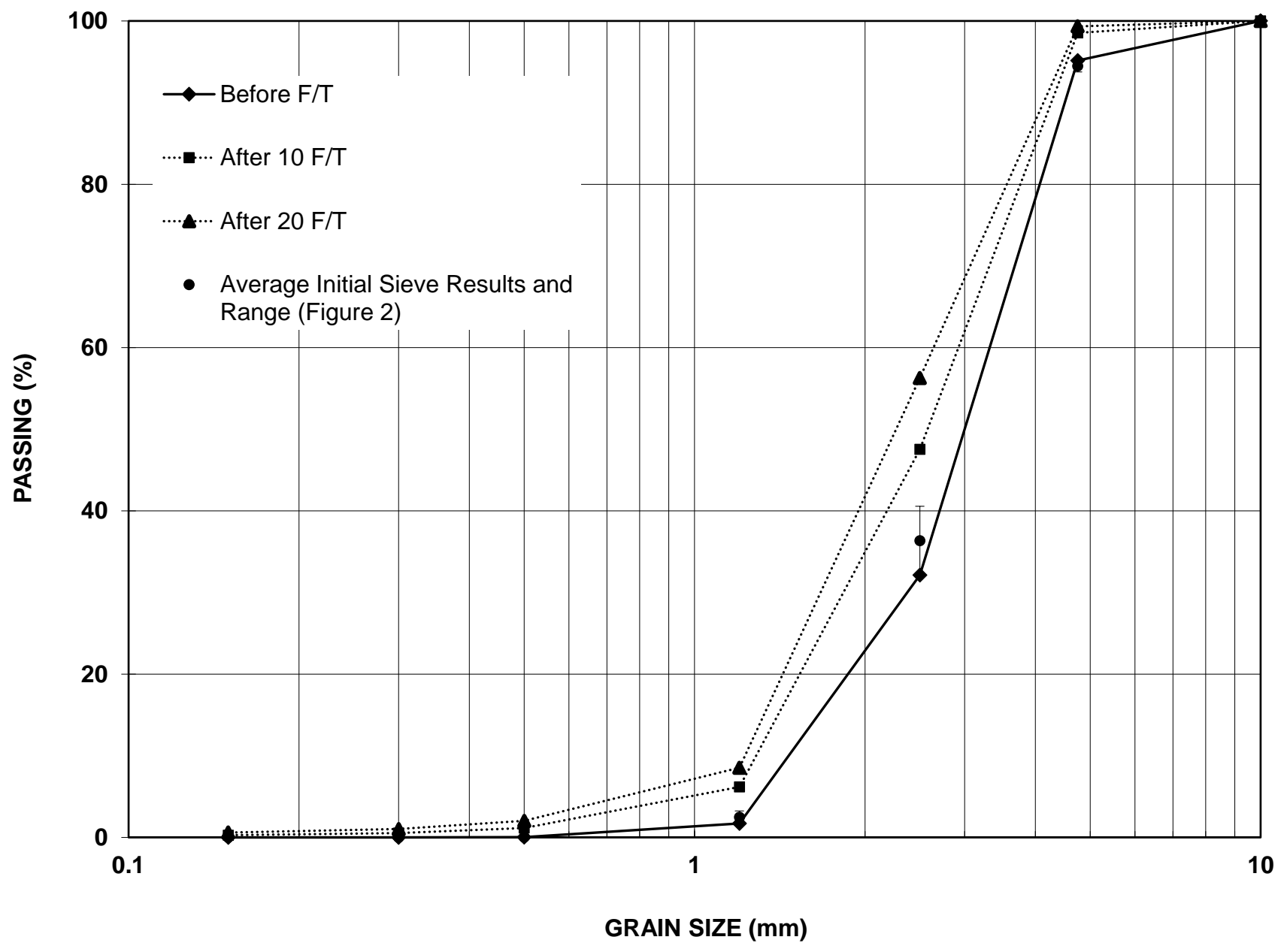


Figure 9

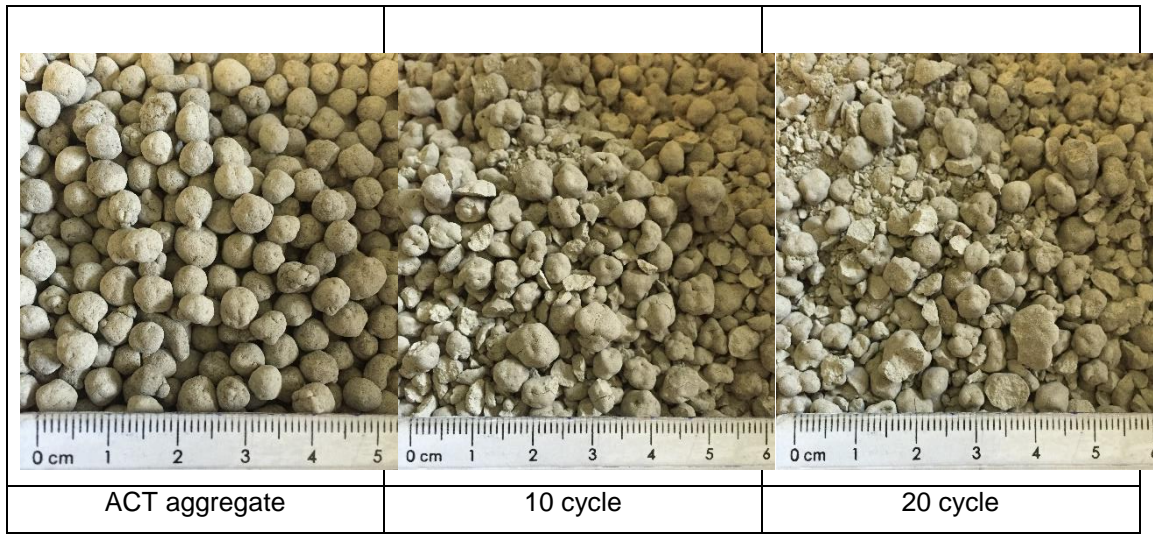


Table 1. Categories and examples of lightweight aggregate (modified from BS EN 13055: BSI, 2016)

<b>Source Material</b>	<b>Lightweight Aggregate Type</b>
Natural Lightweight Aggregate	Pumice, Scoria, Tuff
Manufactured lightweight aggregate from natural source materials	Expanded clay, expanded shale, expanded slate, expanded perlite, expanded vermiculite
Manufactured lightweight aggregate from by-products or recycled source materials	Sintered fly ash, cold-bonded fly ash, foamed blast furnace slag, expanded blast furnace slag, expanded glass, foamed glass
LWA as by-products of industrial processes	Furnace clinker, furnace bottom ash, fly ash

Table 2. Major oxide results for the CKD used in this study.

Oxide	CKD-1 (%)	CKD-2 (%)
CaO	42.2	42.3
SiO <sub>2</sub>	13.1	12.9
K <sub>2</sub> O	5.5	5.5
Al <sub>2</sub> O <sub>3</sub>	3.8	3.8
Fe <sub>2</sub> O <sub>3</sub>	1.3	1.3
MgO	1.1	1.1
Na <sub>2</sub> O	0.3	0.3
TiO <sub>2</sub>	0.2	0.2
P <sub>2</sub> O <sub>5</sub>	0.03	0.3
MnO	0.04	0.05
Cr <sub>2</sub> O <sub>3</sub>	0.01	0.01
V <sub>2</sub> O <sub>5</sub>	< 0.01	< 0.01
LOI	22.4	22.2
SUM	90.0	89.7



Table 3. Elemental analysis for the CKD used in this study\*

Metal	Concentration (mg/kg)		Metal	Concentration (mg/kg)	
	CKD-3	CKD-4		CKD-3	CKD-4
Ag	0.8	0.7	Li	42	42
Al	20470	20800	Mg	6614	6750
Ba	315	310	Mn	329	326
Be	0.6	0.6	Na	2499	2554
Ca	283579	280539	Ni	15	13
Ce	13	13	P	149	150
Co	5	5	Pb	158	156
Cr	10	9	S	43643	43619
Cu	13	11	Sr	355	359
Fe	9275	9058	Ti	1046	1063
K	48887	49380	V	39	39
La	10	10	Zn	19	19
Li	42	42	Zr	27	27

\*Note: As, Bi, Cd, Ga, In, Mo, Nb, Sb, Se, Sn, Ta were below detection limits of the instrument.

Table 4. ACT Derived CKD Aggregate Mix Design and Pelleting Production Process

CKD(g)	Water(g)	Pre-mixing (sec)			Pelleting Time in Drum (min)	Drum Rotation Speed (rpm)
460	130	60 @ 50 rpm	30 @ 120 rpm	90 @ 50 rpm	20	50

Table 5. Grain size, relative density and absorption of ACT derived CKD aggregates

Sub-sample No.	D <sub>10</sub> (mm)	D <sub>30</sub> (mm)	D <sub>60</sub> (mm)	C <sub>u</sub>	C <sub>c</sub>	Group Classification	Relative density* (SSD)	Absorption* (%)
1	1.4	2.0	3.3	2.4	0.9	SP		
2	1.4	2.0	3.3	2.4	0.9	SP	2.1	25.4
3	1.4	2.1	3.3	2.4	1.0	SP		

\*Determined from ASTM (2015).

Table 6. Slake durability test results

Before Test (g)	After First Cycle (g)	After Second Cycle (g)	Slake Durability Index ( $I_d$ ) (%)	Slake Durability Classification (Gamble 1971)
400	397.2	395.3	98.8	Very high durability

Table 7. Leaching test results on ACT aggregate

Metal	Leached Mass per Mass of ACT Aggregate (mg/kg)			% of Average Values of Table 3	Average Leachate Concentrations (ug/L)	Nova Scotia Provincial Guidelines, Tier I Environmental Quality Standards For Groundwater (NSE, 2013)
	ACT-1	ACT-2	ACT-3			(ug/L)
Al	12.9	15.6	23.6	0.1%	1736	-
Ba	0.5	0.5	1.0	0.2%	66	1000
Cr	0.1	0.1	0.1	1.0%	12	25
Cu	0.2	0.3	0.6	3.0%	34	-
Sr	11.8	11.6	12.6	3.4%	1205	4400
Zn	0.2	0.3	0.6	2.0%	38	5000

\*Note: Ag, As, Be, Cd, Co, Mn, Ni, Pb, Sb, Se, Sn, Ti, Tl, and V were below detection limits of the instrument.

Table 8. Single point heavy metal ion batch testing.

Heavy Metal Ions	Concentration of Heavy Metal Ion ( $\mu\text{g/l}$ )		Removal Rate (%)
	Initial Concentration	Final Concentration	
Chromium (Cr)	507.4	38.8	92.4
Zinc (Zn)	546.8	52.0	90.5
Cadmium(Cd)	534.6	1.3	99.8
Arsenic (As)	511.8	20.2	96.0
Lead (Pb)	480.2	4.6	99.0
Copper (Cu)	450.2	27.7	93.8

Table 9. Comparison of Physical Properties of Various Manufactured Aggregates.

	LECA <sup>1</sup>	Lytag <sup>2</sup>	C8A <sup>3</sup>	Poraver <sup>4</sup>	Solite <sup>5</sup>	This study
Description	Lightweight expanded clay	Sintered fly ash	Carbonation stabilised waste	Expanded glass	Expanded shale	ACT Aggregate from CKD
Bulk Density (kg/m <sup>3</sup> )	215-285	750	950-1100	190-400	720-880	1200 (from hydraulic conductivity)
Dry Particle Density	0.4-0.6	1.45	1.94	0.3-0.9	Not specified	2.1 (SSD)
Water Absorption (% by weight)	28	17.5	18.8	14-35	Not specified	25.4
Individual Particle Strength (MPa)	0.89 <sup>6</sup>	3.86 <sup>6</sup>	3.13 <sup>6</sup>	Not specified	Not specified	1.15 <sup>6</sup>

Notes: <sup>1</sup>Weber Saint Gobain (2016); <sup>2</sup>Lytag (2016); <sup>3</sup>Carbon8 (2016); <sup>4</sup>Poraver (2016); <sup>5</sup>Nesolite (2016) <sup>6</sup>Evaluated as part of this study using the methods described in section 2.3.2.1